Available online at www.sciencedirect.com
SCIENCE DIRECT
Journal of Molecular Graphics and Modelling 24 (2006) 254–261
Journal of Molecular Graphics and Modelling
www.elsevier.com/locate/JMGM

Effect of pressure on the conformation of proteins. A molecular dynamics simulation of lysozyme

Andrés N. McCarthy, J. Raúl Grigera *

Instituto de Física de Líquidos y Sistemas Biológicos (IFLYSIB), CONICET-UNLP-CIC, and Departamento de Ciencias Biológicas, Facultad de Ciencias Exactas, Universidad Nacional de La Plata, 49-789 cc 565, B1900BTE La Plata, Argentina

Received 7 April 2005; received in revised form 18 September 2005; accepted 20 September 2005
Available online 21 October 2005

Abstract

The effect of pressure on the structure and mobility of lysozyme was studied by molecular dynamics computer simulation at 1 and 3 kbar (1 atm = 1.01325 bar = 101.325 kPa). The results have good agreement with the available experimental data, allowing the analysis of other features of the effect of pressure on the protein solution. The studies of mobility show that although the general mobility is restricted under pressure this is not true for some particular residues. From the analysis of secondary structure along the trajectories it is observed that the conformation under pressure is more stable, suggesting that pressure acts as a 'conformer selector' on the protein. The difference in solvent-accessed surface (SAS) with pressure shows a clear inversion of the hydrophilic/hydrophobic SAS ratio, which consequently shows that the hydrophobic interaction is considerably weaker under high hydrostatic pressure conditions.

Keywords: Pressure; Protein; Lysozyme

1. Introduction

Pressure has long been used as an experimental variable in physicochemical studies of systems in equilibrium, although its role in studies of bio-systems in general has not been as extensively exploited. Recent advances in structural and analytical studies of protein solutions under high pressure have opened new highways for research in this area [1,2]. Consequently, pressure is regarded today as an important variable for studying protein structure–function relationships [3]. The thermodynamic principle governing changes in a system in equilibrium is given by:

$$\left(\frac{\partial \ln K}{\partial P}\right)_T = -\left(\frac{\Delta V}{RT}\right) \quad (1)$$

This makes clear that an increase in pressure will shift the equilibrium of the system toward the state with the lowest overall volume.

Historically pressure has been regarded as a potential denaturant of proteins, among other effects. However, in relation to chemical and thermal denaturation, pressure offers a unique feature: this denaturation process has been found to be predominantly reversible for a wide range of high hydrostatic pressures [4]. This observation constitutes a major affirmation, taking into account that we are thus able to apply equilibrium thermodynamics to analyse denaturation — a process regarded generally as irreversible. It has been established that pressure has also important effects on protein structure and mobility [4,5].

Oligomeric assemblies separate in their constituent monomers with moderate pressure increase [4], process that has been found to present an important degree of reversibility in most cases [2,4,6]. Concomitantly, partial loss in the tertiary structure of monomers has been observed [7,8]. On the other hand, the effect of pressure on the mobility of proteins does not offer straightforward results. Some proteins have been observed to increase their general mobility [9], whilst others manifest a notorious decrease with high hydrostatic pressure [5,10–12].

Recent studies have advanced greatly in elucidating the nature and behaviour of many intra and intermolecular interactions such as the effects on salt bridges (electrostriction) [13–16] or the shortening of hydrogen bonds [17–20]. Nevertheless, advances in studies of the stabilising effects of cryosolvents on protein native structure [21–26], as well as the mobility issue pointed out previously [9,10], also prove that hydration cannot be solely explained by a single water exclusion model [27]. These results

* Corresponding author. Tel.: +54 221 423 32 83; fax: +54 221 425 73 15.
E-mail address: grigera@iflysib.unlp.edu.ar (J.R. Grigera).

1093-3263/$ – see front matter
doi:10.1016/j.jmgm.2005.09.007

clearly call for the elaboration of more complete and comprehensive hydration models.

Furthermore, a strong controversy still remains as to how pressure affects hydrophobic interactions. Present literature exposes the existence of antagonizing theories in relation to this issue [28–32]. While some propose a general reduction of the hydrophobic effect with the rise in pressure, due mainly to the effects of pressure on the solvent–protein system [30,31], others state that the formation of clathrates around hydrophobic residues, being a process that involves a positive ΔV for the system, is negatively selected as the solvent–protein system shifts to lower overall volume states with the rise in pressure (see Eq. (1)). Consequently the hydrophobic interactions should be enhanced, rather than reduced, at higher pressures [27–29].

It is at this point where having a molecular perspective of the problem can prove to be of great value in bringing some light on the problem of changes in intra and intermolecular interactions with pressure, especially in relation to the hydrophobic effect and its behaviour.

Thousands of protein structures are readily available from the Protein Data Banks as a direct consequence of the exponential advance in macromolecular structure resolution technology. We have taken particular interest, for this study, in 2D-NMR techniques developed to resolve protein structures in solution, and lately also applied to systems under high hydrostatic pressure [33].

Molecular dynamics simulations have been already used to obtain detailed information on the effect of high pressure on proteins [34–36]. However, the time span covered by these studies was in the range of a few hundred picoseconds, which precludes the description of a phenomenon that takes place in a much larger time scale [37].

The NMR-refined structure of hen egg white lysozyme (1GXV) was chosen as the starting point for our molecular dynamics simulation (MD).

The results produced by MD are in qualitative accordance with the experimental data recently published [38]. This allows us to assertively analyse the kinetic data produced by the MD simulations such as mobility, solvent accessible surface, as well as specific residue solvent interactions and hydration, among other data.

We hereby present a MD Simulation method for studying the properties of proteins in solution, using pressure as a thermodynamic variable, making it feasible to screen through the conformational ensemble of proteins in solution, and ultimately allowing us to achieve some insight on the molecular mechanisms of the unfolding process.

2. Materials and methods

We carried out the molecular dynamic (MD) simulations using the GROMACS 3.2.1 package [39,40] in which the equations of motion are solved using a leap-frog integration step. We used all atoms (ff2gmx) force field [41–46] for the minimization process, as well as for all the MD simulation steps and kept all protein bond lengths constrained using the LINCS algorithm [47]. Water molecules were constrained using the SETTLE algorithm [48]. For the calculation of electrostatic forces we applied the Reaction Field method [49]. Lennard–Jones interactions were calculated within a cut-off radius of 1.4 nm.

For all the simulation runs we have used a Pentium III-based, 4-processor cluster, running under GNU/Linux and for all plots and graphics MS Windows or GNU/Linux, using the reference Visual Molecular Dynamics package, Swiss PDB Viewer or XGrace software.

As starting configurations we have used the high and low pressure NMR-structure of hen egg white lysozyme [38] (PDB codes 1GXX and 1GXV, respectively) readily available at the Protein Data Bank and generated the topology using the PDB2GMX tool, with standard pH 7 aminoacid protonation states. The SPC/E [50] water model was used for both high and low pressure systems. The starting system consisted of a cubic simulation box of $X = Y = Z = 4.9588$ nm, with a total volume of 121.9354 nm^3, containing one lysozyme molecule and 3497 water molecules.

This system was energy minimized using firstly the steepest descent method, converging to machine precision. Secondly, the conjugated gradient method was applied, converging in less than 20 cycles. After this, the solvent was allowed to relax running a short 10 ps MD simulation with position restraints applied on all the protein atoms.

At the beginning the system was weakly coupled to a thermal and hydrostatic bath, in order to work in the isothermal-isobaric ensemble [51] at $T = 315$ K and $P = 1$ bar. Subsequently, the whole system was allowed to relax (restraints were removed from all atoms) during 200 ps, coupled to the same weak thermal and hydrostatic bath.

At this point we divided the system in two. The first copy was slowly submitted to increasing hydrostatic pressure, whilst the second was kept at atmospheric pressure.

The pressure in the first system was elevated in 22 concatenated runs during a total 4.4 ns as follows: 1–10 bar, during 200 ps; 10–100 bar, during 200 ps; 100–1000 bar (100 bar increase during 200 ps for each run); 1000–3000 bar (200 bar increase during 200 ps for each run). The second system was allowed to run for an equivalent 4.4 ns MD simulation period at 1 bar.

Having reached this point we allowed both systems to evolve during 8 ns each, in order to produce comparably equilibrated starting points for the low and high pressure systems.

Once this was achieved, we made 24 ns MD simulation for both the 1 and 3 kbar systems. All of the subsequent analysis corresponds to the data produced by these 24 ns long MD simulations.

3. Results and discussion

3.1. Low and high pressure average structures comparison

Fig. 1 shows the difference of the distance between the α-carbon of each aminoacid with the rest at low and high

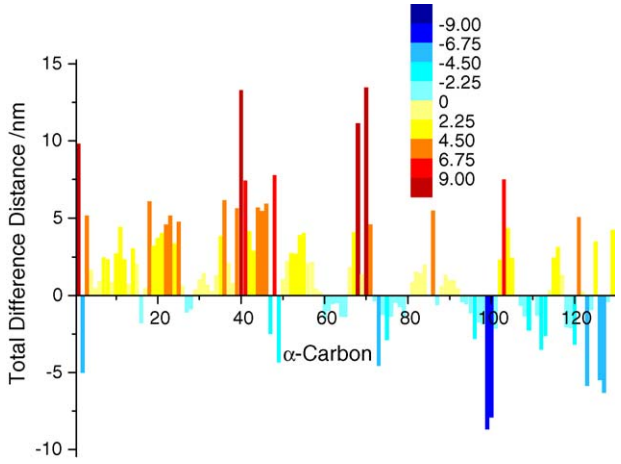

Fig. 1. Difference of the distance between the α-carbon of each aminoacid with the rest at low and high pressure average configurations.

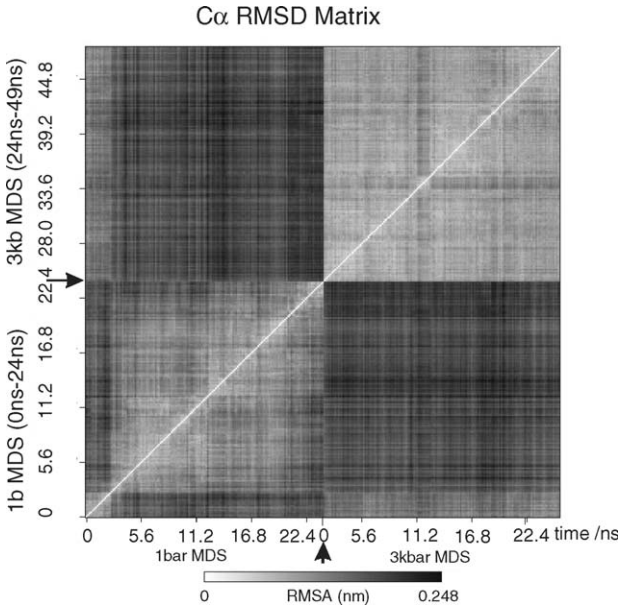

Fig. 2. Matrix for the α-carbon positional root mean square deviation (R.M.S.D.) of the low and high pressure trajectories, after a least-square fit of each pair. The arrows indicate the starting point of the high pressure run, as well as the end of the low pressure run.

pressure average configurations. Positive differences indicate that in the high pressure structure the atoms come closer to each other. In the first place most α-carbons come closer to the rest (red tones), which means that the general structure becomes more compact.

On the other hand, notably, other α-carbons move away from their pairs (blue tones), which indicates that, although there appears to be a general compression, certain specific residues move out of the structure.

This result is in qualitative accordance with the experimental low and high pressure NMR structural readily available data [38].

Although this last statement is true for most residues, there are certain exceptions to this general behaviour.

The experimental data, available both by high pressure NMR [38] and crystallography [52], shows a general compression around residue 100 and an expansion mainly at residues 61–87. The MD simulation shows a less homogenous behaviour at residues 61–87, although the expansion peak remains unchanged at residue 73. The general expansion observed through MD around residue 100 is probably establishing the limits of the present MD study. Namely, that the results presented in this manuscript are in good qualitative general accordance with experiment when analysing the system on the entire protein scale.

3.2. Low and high pressure general structure R.M.S.D. screening

For a general screening of possible structural similarities or differences during the simulations we have calculated the matrix for the α-carbon positional root mean square deviation (R.M.S.D.) of every frame against every other frame (after a least-square fit performed for each pair) of the low and high pressure trajectories.

The results are presented in Fig. 2, in grey-coded format. White corresponds to R.M.S.D. = 0 nm, whilst black must be interpreted as R.M.S.D. $\geq$ 0.248 nm.

As a first observation, it is clear that the high pressure system shows a much greater general homogeneity throughout the simulation run, as compared to the low pressure system's behaviour.

This result is also in very good accordance with the experimental data available, regarding the effects of pressure on the structural transitions of hen egg white lysozyme [53].

It is also worth noting that there are, almost evenly distributed throughout the low pressure trajectory, a few structures which could be compatible with the more homogenous high pressure conformers.

3.3. Secondary structure analysis

Figs. 3 and 4 show, respectively, the secondary structure (SS) total count for the low and high pressure runs analysed

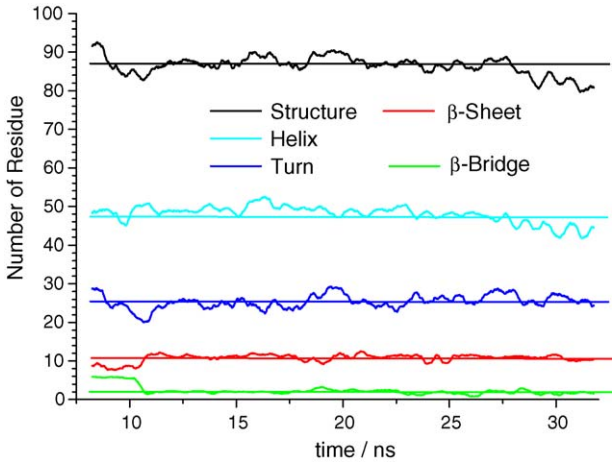

Fig. 3. Secondary structure along the simulation trajectory at 1 bar according to the definition of the Dictionary of Secondary Structure in Proteins (Ref. [44]).

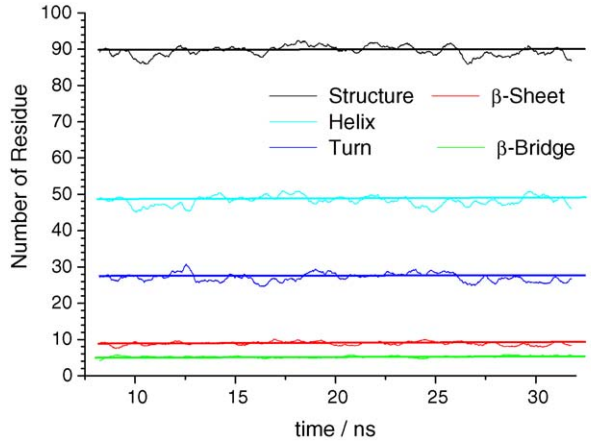

Fig. 4. The same as Fig. 3 for 3 kbar trajectories.

according to the reference definitions used in the Dictionary of Secondary Structure in Proteins [54].

In Figs. 5 and 6, detailed information is presented as to how each residue participates of the proteins secondary structure, as well as the evolution of such a property during each run.

A first general comparison of both graphs confirms the impression obtained by the R.M.S.D. matrix screening that, in the case of lysozyme, the secondary structure fluctuations are highly reduced with the increase in pressure, hence augmenting the structural homogeneity of the system. Likewise, it can also be observed that the total structural count (calculated as α-helix + β-sheet + β-bridge + turn) increases, and is also stabilised, significantly with pressure.

A more detailed study of Figs. 3 and 4 reveal the fact that the prevalent structure during roughly the first 2,2 ns of the low pressure run is largely compatible with the average structure which is stabilised during most of the high pressure run. This is mostly noted when focusing on the β-sheet and -bridge secondary structures.

This last observation is highly compatible with the conformer selection role of pressure, proposed in recent publications [1].

On the whole, it may be said that this complimentary and more detailed information confirms the previous conclusions regarding the structural variability difference between the low and high pressure MD runs.

It can be clearly concluded from a first analysis of these figures that many residues show grater variability in the type of structures they adopt throughout the simulation at low pressure when compared with the high pressure run.

We are also able to observe that, although most residues keep their low pressure secondary structure, notably others manifest a significant shift. Good examples of this are residues 2–3, 20, 23 and 39, which adopt a permanent β-bridge structure at high pressure when this is not at all the most significant structure for these residues at low pressure.

Nevertheless it is also important to note that, although in a much reduced proportion, for every residue the prevalent secondary structure at high pressure is also present during the low pressure run.

In the light of Figs. 5 and 6 it can be seen that the structure stabilised at high pressure corresponds to conformers that can also be observed at low pressure, although they are by no means prevalent under the latter conditions.

3.4. Mobility analysis

In order to analyse the relative mobility of the atoms of the protein at low and high pressure we have computed the R.M.S.F. of α-carbon atoms under both situations. Fig. 7 shows the average R.M.S.F. for the full run for each pressure. It can be seen that that the average residue mobility is significantly decreased with high pressure.

There are, nonetheless, certain residues whose mobility increases. Such is the case of the superficial Asp 18, 48, 87, and 119.

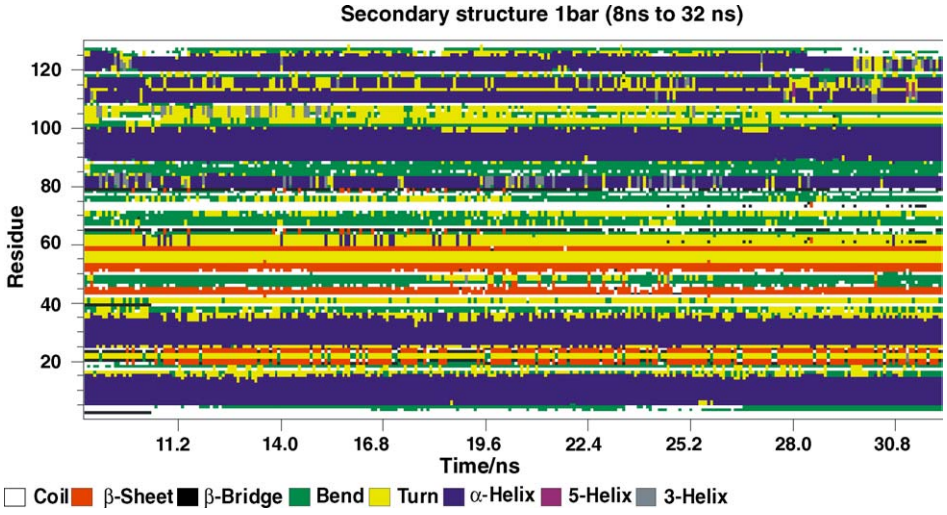

Fig. 5. Detailed secondary structure data for each residue along the complete trajectory (24 ns) at 1 bar.

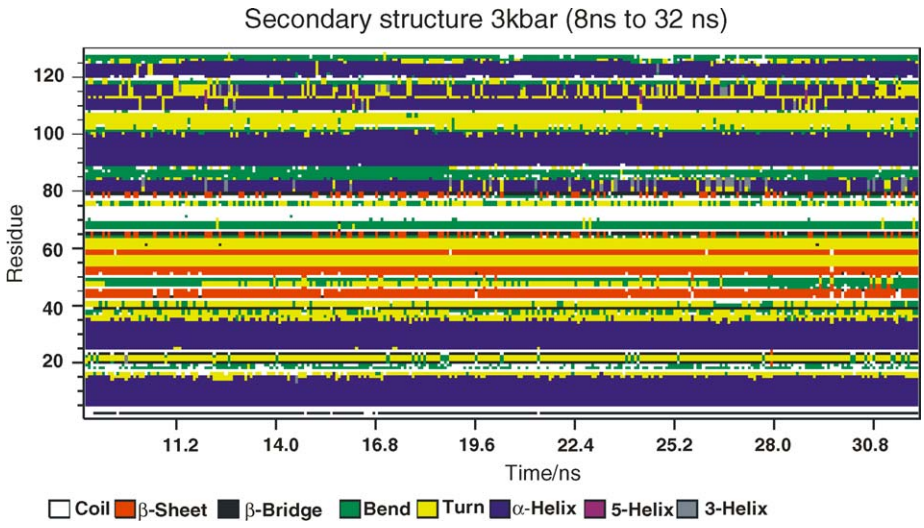

Fig. 6. The same as Fig. 5 for the simulation at 3 kbar.

To analyse the possible case of such behaviour we have computed the radial distribution functions (RDF) of water oxygen around the carbonil oxygen atoms of the residues that increase their mobility. This is shown in Fig. 8.

We can observe in Fig. 8 (a–c) that at high pressure the second hydration layer around the residues 18, 48, and 87 is reduced in relation to the low pressure situation. The reduction of the hydration layer may favour residue mobility.

However, this reasoning cannot be applied to the results obtained for Asp 119 (Fig. 8d), where we see a slightly bigger hydration layer when pressure is applied. We must remember that the radial distribution function does not describe the hydrogen bonded water molecules but the number of waters surrounding the atom. It may happen that the pressure produces an increment of the number of water molecules but in a different arrangement which allows higher mobility. This speculation cannot be proved without a careful analysis of the hydrogen bond network around the residue, which remains yet to be done.

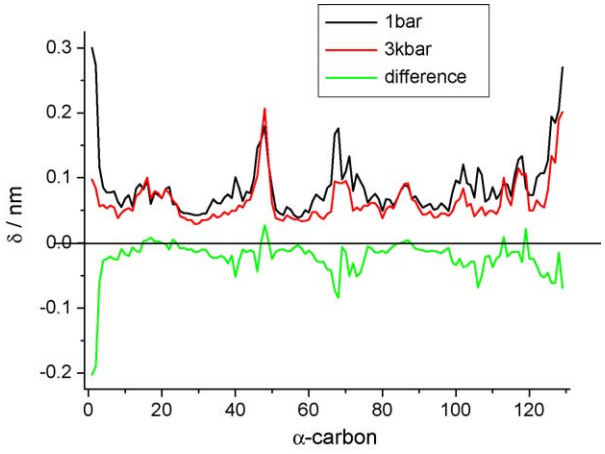

Fig. 7. Average R.M.S. fluctuation of α-carbon atoms at 1 bar and 3 kbar and its difference.

The general reduction in the mobility of certain globular proteins – kept under the molten globule transition state – with the increase in pressure is a widely observed experimental fact [5,9–11], and is in accordance with the mentioned experimental data available for lysozyme [53].

We have therefore been able to reproduce not only the experimental average structural information but also the dynamic behaviour that has been recently assigned to lysozyme in solution under high pressure.

These results, together with all the previously mentioned accordance between the available experimental data and our molecular dynamics simulation calculations, allows us, at this point, to assertively establish that an important degree of correlation exists between the model and the real system.

3.5. Solvent accessible surface analysis (SAS)

Fig. 9 shows the solvent-accessed surface (SAS) for hydrophilic and hydrophobic residues of lysozyme at 1 bar, while Fig. 10 shows the corresponding graphic for 3 kb.

This SAS (Connelly's surface) is computed as the area exposed to a spherical probe of 0.14 nm radius, and was calculated using the g_sas program [55].

We observe that at low pressure (Fig. 9) the hydrophilic SAS is predominant over the hydrophobic SAS, results that are expected in a regular situation in which hydrophobic residues avoid contact with water. On the contrary, at high pressure this behaviour is reversed.

The relative increase in the number of non-polar residues in contact with the solvent at high pressure indicates loss of the regular behaviour of hydrophobic substances in water. As pressure has no effect on the direct interactions the answer must be the, at least partial, loss of the hydrophobic effect, which could be readily explained by the reduction of the degree of structure present in the bulk of the water under pressure [56].

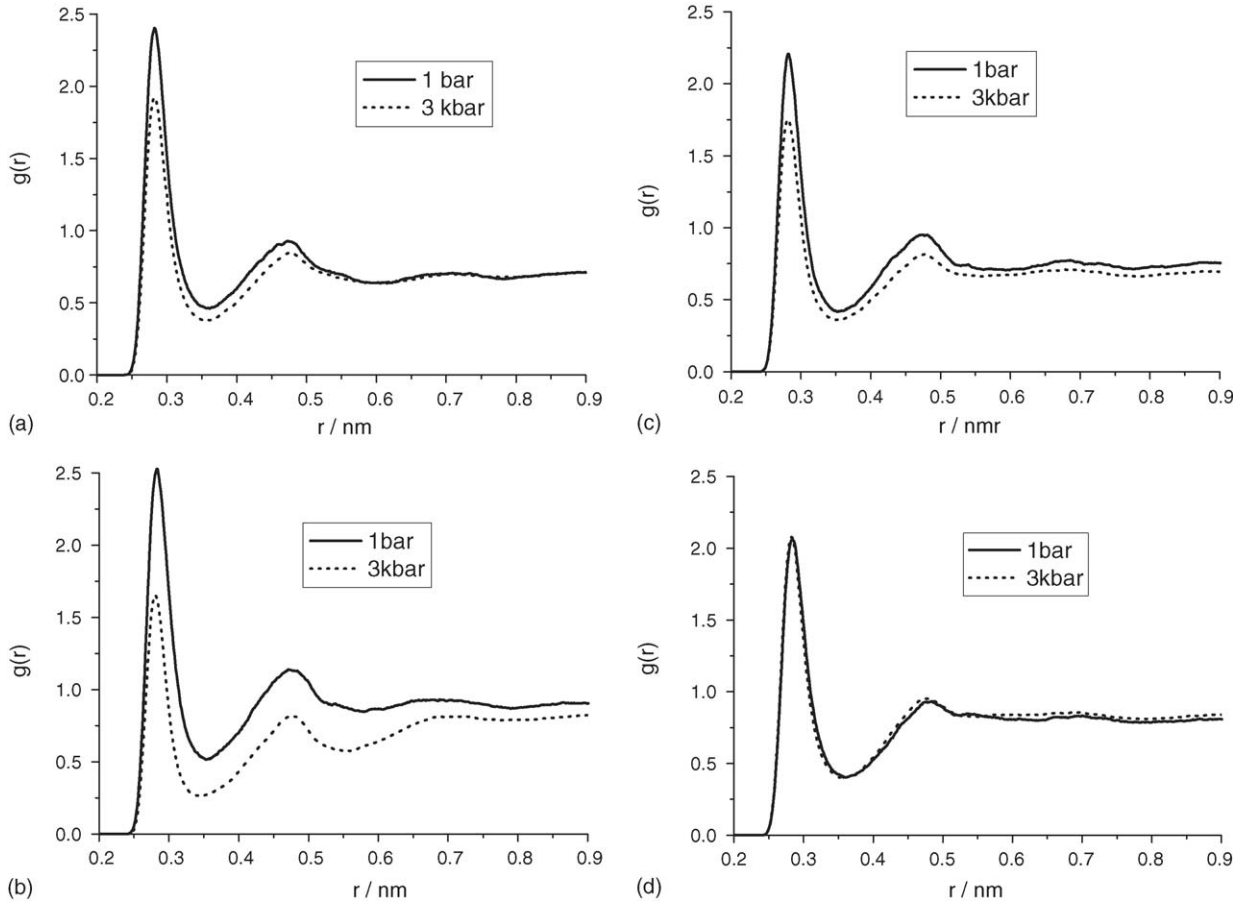

Fig. 8. Radial distribution functions of the water oxygen around the mobile Asp residues at 1 bar and 3 kbar: (a) Asp18; (b) Asp48; (c) Asp87; (d) Asp119. The radial distribution function $g(r)$ is the density of probability of finding a particle at distance r from the reference particle, normalised to a probability equal to 1 at large r.

Nevertheless, an important variability can be pointed out in the results shown in Fig. 9. Notably, certain periods can be clearly observed in which the hydrophilic/hydrophobic SAS ratio is inverted. As we compare this aspect with the graph shown in Fig. 10, a decrease of roughly 1 nm^2 can be observed for both the hydrophilic and the hydrophobic maximum and minimum values. This, analysed in the light of the previous data presented, reinforces the conclusion that, in the case of lysozyme, pressure acts as an effective conformer selector, consequently reducing the structural variability.

The effect of pressure on the water structure is clearly reflected on the weakness of the hydrogen bond network [57]. This situation would clearly reduce the hydrophobic effect.

It is therefore sensible to expect a hydrophobic residue to be more easily exposed to a less-structured solvent, which would

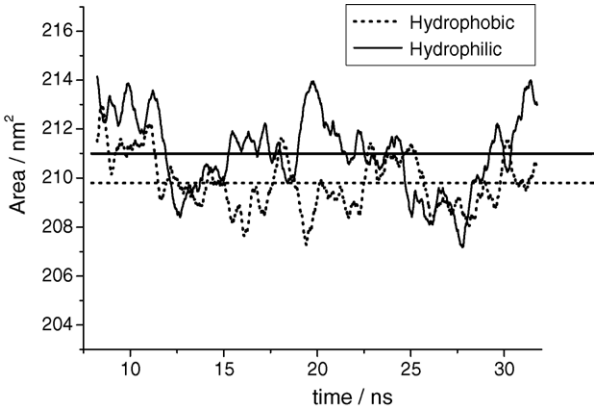

Fig. 9. Hydrophilic and hydrophobic solvent accessible area (SAS) against the simulation time at 1 bar. The horizontal lines show the average value over the complete run.

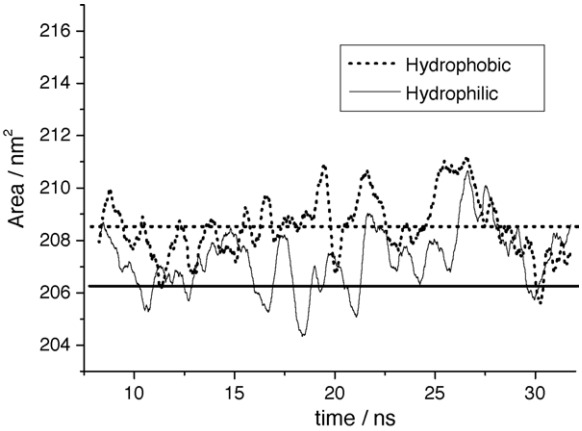

Fig. 10. The same as Fig. 9 for 3 kbar.

consequently constitute the main driving force for pressure driven protein denaturation.

4. Conclusions

The present model not only reproduces the global behaviour of lysozyme under pressure, but also is able to account for the apparently anomalous behaviour of certain specific protein regions — as described by recent experimental results. Namely, the model is successful in showing a global increase in com-pactness under pressure, as well as correctly describing the beha-viour of the few regions which recently have been described as moving out of the structure under the effects of high hydrostatic pressure.

We have also been successful in reproducing the increase in general structural homogeneity under pressure. In this sense, as we focus on specific structural elements such as regional secondary structure fluctuations, new microscopic elements arise which offer us independent arguments that point in the direction of confirming the recently proposed ''conformer selection'' role of pressure for proteins in solution.

Regarding the protein mobility study, a first direct observation of the results offered by these MD Simulations confirms the previous statements as to the effects of pressure in producing a general decrease in the structural degrees of freedom of this protein in solution.

Although the issue of offering a full explanation for the apparently anomalous increase in mobility for the charged external residues still remains unsolved, a first preliminary approach seems to point in the direction of the change in the hydration sphere of these residues as an important factor that could explain this behaviour.

The evaluation of the difference in solvent-accessed surface (SAS) with pressure increase shows a clear inversion of the hydrophilic/hydrophobic SAS ratio, difference which is dynamically sustained throughout the entire MD simulation time. This ratio inversion alone constitutes the most remarkable parameter shift, as regards pressure-induced changes, for the whole system. This difference must be interpreted as a decrease in the hydrophobic effect with the rise in pressure, which would reasonably be expected to account for most of the driving force involved in pressure-induced protein unfolding.

Acknowledgements

This work was partially supported by the Consejo Nacional de Investigaciones Científicas y Técnicas of Argentina (CONICET), the University of La Plata, the Comisión Científica de la Provincia de Buenos Aires (CIC) and the Agencia Nacional de Promoción Científica y Tecnológica de Argentina (ANPCyT). JRG is member of the Carrera de Investigador of CONICET. ANMC is founded by ANPCyT.

References

[1] K. Akasaka, Biochemistry 42 (2003) 10875–10885.
[2] V.V. Mozhaev, K. Heremans, J. Frank, P. Masson, C. Balny, Protein Struct. Funct. Genet. 24 (1996) 81–91.
[3] C.R. Robinson, S.G. Sligar, Meth. Enzymol. 259 (1995) 395–426.
[4] M. Gross, R. Jaenicke, Eur. J. Biochem. 221 (1994) 617–630.
[5] M.M.C. Sun, N. Tolliday, C. Vetriani, F.T. Robb, D.S. Clark, Protein Sci. 8 (1999) 1056–1063.
[6] J.L. Silva, D. Foguel, A.T. Da Poian, P.E. Prevelige, Curr. Opin. Struct. Biol. 6 (1996) 166–175.
[7] J.L. Silva, C.F. Silveira, A. Correira, L. Pontes, J. Mol. Biol. 223 (1992) 545–555.
[8] X. Peng, J. Jonas, J.L. Silva, Biochemistry 33 (1994) 8323–8329.
[9] N. Tanaka, C. Ikeda, K. Kanaori, K. Hiraga, T. Konno, S. Kunugi, Biochemistry 39 (2000) 12063–12068.
[10] N. Tanaka, D. Mitani, S. Kunugi, Biochemistry 40 (2001) 5914–5920.
[11] P. Cioni, G.B. Strambini, J. Mol. Biol. 242 (1994) 291–301.
[12] G. Wagner, FEBS Lett. 112 (1980) 280–284.
[13] S.D. Hamann, Rev. Phys. Chem. Jpn. 50 (1980) 147–168.
[14] T.V. Chalikian, A.P. Sarvazyan, K.J. Breslauer, J. Phys. Chem. 97 (1993) 13017–13026.
[15] A. Disteche, Symp. Soc. Exp. Biol. 26 (1972) 27–60.
[16] A. Disteche, Symp. Soc. Exp. Biol. 26 (1972) 27–60.
[17] J.W. Linowski, N.-I. Liu, J. Jonas, J. Chem. Phys. 65 (1976) 3383–3384.
[18] J.W. Linowski, N.-I. Liu, J. Jonas, J. Magn. Reson. 23 (1976) 455–460.
[19] K. Goossens, L. Smeller, K. Heremans, J. Chem. Phys. 99 (1993) 5736–5741.
[20] H. Li, H. Yamada, K. Akasaka, Biochemistry 37 (1998) 1167–1173.
[21] K. Gekko, S.N. Timasheff, Biochemistry 20 (1981) 4667–4676.
[22] A. Priev, A. Almagor, S. Yedgar, B. Gavish, Biochemistry 35 (1996) 2061–2066.
[23] V. Mozhaev, R. Lange, E.V. Kudryashova, C. Balny, Biotechnol. Bioeng. 52 (1996) 320–331.
[24] M.J. Kornblatt, J.A. Kornblatt, G. Hui Bon Hoa, Arch. Biochem. Biophys. 306 (1993) 495–500.
[25] J.A. Kornblatt, G. Hui Bon Hoa, Biochemistry 29 (1990) 9370–9376.
[26] M.M.C. Sun, R. Caillot, G. Mak, F.T. Robb, D.S. Clark, Protein Sci. 10 (2001) 1750–1757.
[27] B.B. Boonyaratanakornkit, C.B. Park, D.S. Clark, Biochim. Biophys. Acta 1595 (2002) 235–249.
[28] D.J. Hei, D.S. Clark, Appl. Environ. Microbiol. 60 (1994) 932–939.
[29] P.C. Michels, D. Hei, D.S. Clark, Adv. Protein Chem. 48 (1996) 341–376.
[30] W. Kauzmann, Nature 325 (1987) 763–764.
[31] K.J. Frye, C.A. Royer, Protein Sci. 7 (1998) 2217–2222.
[32] G. Hummer, S. Garde, A.E. García, M.E. Paulaitis, R. Pratt, Biophysics 95 (1998) 1552–1555.
[33] Y.O. Kamatari, R. Kitahara, H. Yamada, S. Yokoyama, K. Akasaka, Methods 34 (2004) 133–143.
[34] D.B. Kitchen, L.H. Reed, R.M. Levy, Biochemistry 31 (1992) 10083–10093.
[35] E. Paci, M. Marchi, J. Phys. Chem. 100 (1996) 4314–4322.
[36] R.M. Brunne, W.F. van Gunsteren, FEBS Lett. 323 (1993) 215–217.
[37] P.E. Hunenberger, A.E. Mark, W.F. van Gunsteren, Proteins 21 (1995) 196–213.
[38] M. Refaee, T. Tezuka, K. Akasaka, M.P. Williamson, J. Mol. Biol. 327 (2003) 857–865.
[39] E. Lindahl, B. Hess, D. van der Spoel, J. Mol. Mod. 7 (2001) 306–317.
[40] H.J.C. Berendsen, D. van der Spoel, R. van Drunen, Comput. Phys. Commun. 91 (1995) 43–56.
[41] W.F. van Gunsteren, H.J.C. Berendsen, Biomos BV Nijenborgh 4, 9747 AG Groningen, the Netherlands, 1987.
[42] A.R. van Buuren, S.J. Marrink, H.J.C. Berendsen, Phys. Chem. 97 (1993) 9206–9212.
[43] A.E. Mark, S.P. van Helden, P.E. Smith, L.H.M. Janssen, W.F. van Gunsteren, Am. Chem. Soc. 116 (1994) 6293–6302.
[44] W.L. Jorgensen, J. Chandrasekhar, J.D. Madura, R.W. Impey, M.L. Klein, J. Chem. Phys. 79 (1983) 926–935.
[45] A.R. van Buuren, H.J.C. Berendsen, Biopolymers 33 (1993) 1159–1166.

[46] H. Liu, F. Müller-Plathe, W.F.J. van Gunsteren, Am. Chem. Soc. 117 (1995) 4363–4366.
[47] B. Hess, H. Bekker, H.J.C. Berendsen, J.G.E.M. Fraaije, J. Comput. Chem. 18 (1997) 1463–1472.
[48] S. Miyamoto, P.A. Kollman, J. Comput. Chem. 13 (1992) 952–962.
[49] I.G. Tironi, R. Sperb, P.E. Smith, W.F. van Gunsteren, J. Chem. Phys. 102 (1995) 5451–5459.
[50] H.J.C. Berendsen, J.R. Grigera, T.P.J. Straatsma, Phys. Chem 91 (1987) 6269–6271.
[51] H.J.C. Berendsen, J.P.M. Postma, A. DiNola, J.R. Haak, J. Chem. Phys. 81 (1984) 3684–3690.
[52] C.E. Kundrot, F.M.J. Richards, J. Mol. Biol. 193 (1987) 157–170.
[53] K. Sasahara, M. Sakurai, K. Nitta, Protein Struct. Funct. Genet. 44 (2001) 180–187.
[54] W. Kabsch, C. Sander, Biopolymers 22 (1983) 2577–2637.
[55] Frank Eisenhaber, Philip Lijnzaad, Patrick Argos, Chris Sander, Michael Scharf, J. Comp. Chem. 16 (1995) 273–284.
[56] M.A. Anisimov, J.V. Sengers, J.M.H. Levelt Sengers, in: D.A. Palmer, R. Fernández-Prini, A.H. Harvey (Eds.), Physical Chemistry in Water, Steam and Hydrothermal Solutions, Elsevier, Amsterdam, 2004.
[57] E.R. Caffarena, J.R. Grigera, Physica A 342 (2004) 34–39.